Optimal quantum search on truncated simplex lattices

Yunkai Wang,[1,2,3] Shengjun Wu,[1,4,*] and Wei Wang[1,4,†]

[1]*Institute for Brain Sciences and Kuang Yaming Honors School, Nanjing University, Nanjing 210023, China*
[2]*School of Astronomy and Space Science, Nanjing University, Nanjing 210023, China*
[3]*Department of Physics, University of Illinois at Urbana-Champaign, Urbana, Illinois 61801, USA*
[4]*National Lab of Solid State Microstructure, Collaborative Innovation Center of Advanced Microstructures, and Department of Physics, Nanjing University, Nanjing 210093, China*

(Received 3 December 2019; accepted 3 June 2020; published 24 June 2020)

First-order truncated simplex lattices have been used as interesting data structures to explore the properties of quantum search such as the effect of connectivity on search speed [D. A. Meyer and T. G. Wong, Phys. Rev. Lett. **114**, 110503 (2015)]. In this paper, we further discuss quantum search algorithms for truncated simplex lattices. We first propose a multistage quantum algorithm for an rth-order truncated simplex lattice with N vertices based on the numerical calculation up to the fifth-order lattice, which requires an $(r+1)$-stage search process and consumes a run time $\Theta(N^{(2r+1)/(2r+2)})$ in general. Furthermore, with edge weights suitably adjusted (which increases the connectivity according to certain definitions), we merge the multistage search process into a single stage and achieve a fast quantum search algorithm with an optimal run time $\Theta(\sqrt{N})$ for first-order truncated simplex lattices, which we conjecture is generally true for any-order lattice. Under small noise of the lattice structure, both our multistage and our single-stage search algorithms are quite robust.

DOI: 10.1103/PhysRevA.101.062333

I. INTRODUCTION

As one of the first examples of lattices with effectively noninteger dimensionality [1], truncated simplex lattices are of great interest in several fields. Self-avoiding walks, which are classical random walks with the constraint that any lattice vertices cannot be visited more than once, on truncated simplex lattices are discussed to model several problems [2–7]: some solvable cases of self-avoiding random walks on truncated simplex lattices [2], the collapse transition of linear polymers on truncated simplex lattices [3], two interacting chemically different linear polymer chains on a truncated simplex lattice, to study critical behavior [4], and the effect of interpenetration of chains [5–7]. Space-time of noninteger dimensionality on truncated simplex lattices is discussed [8]. Quantum search on the truncated simplex lattice has also attracted a lot of interest recently [9–13].

The spatial search problem aims at searching for one of the marked vertices on a graph, which is equivalent to searching for one of the marked items in a structured database. Classically, this problem could be solved by applying the random walk repeatedly until reaching one of the marked vertices. The quantum walk, the analog of the classical random walk, has been proposed as a tool in many fields of science [14–16]. Several aspects of the discussion related to quantum walks are listed: computational universality of the quantum walk [17–19], the quantum walk as a tool to design a quantum algorithm [20,21], simulation of photosynthetic processes based on the quantum walk [22], exploration of the foundation of quantum theory [23,24], and topological properties of the system [25,26]. Using the continuous-time quantum walk (CTQW), Childs and Goldstone solved the spatial search problem on complete graph, hypercube, and d-dimensional periodic lattices [9]. Compared to the well-known Grover's algorithm for search in an unstructured database [27], quantum search via CTQW is intended for search in a physical database that has structures.

Since the scheme was first proposed, quantum search via CTQW has been discussed for several types of graphs: strongly regular graphs [28], first-order truncated M-simplex lattices [10], balanced trees [29], Erdös-Renyi random graphs [30], complete bipartite graphs, star graphs [31], Johnson graphs [32], dual Sierpinski gaskets, T fractals, and Cayley trees [33]. The properties of quantum search via CTQW have been further investigated. Connectivity, global symmetry, and regularity are shown to be poor and unnecessary indicators for faster search [10,28,31]. The importance of topological arrangements of graphs is pointed out [33]. Quantum walks on weighted graphs have been discussed for several topics [11,12,34–36]. In particular, it is shown that by engineering the weight of edges of a graph, one can speed up the search process [12] and increase the success probability [11].

We focus on quantum search via CTQW on truncated simplex lattices. The zeroth-order truncated simplex lattice is just the complete graph, which has been discussed in Ref. [9]. The first-order truncated simplex lattice has been used to provide a counterintuitive example to show that connectivity is a poor indicator for faster search [10], explore quantum search with multiple walk steps per oracle query [37] and with multiple marked vertices [13], and discuss quantum search on weighted graphs [11,12]. Despite the rich properties exhibited on truncated simplex lattices so far, a general theory of the

*sjwu@nju.edu.cn
†wangwei@nju.edu.cn

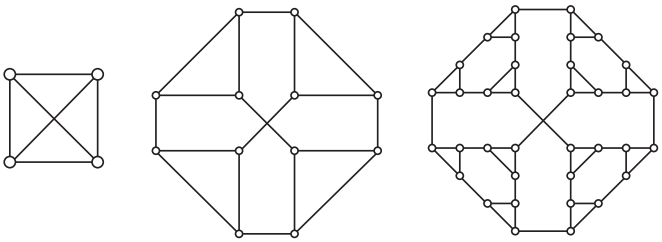

FIG. 1. Zeroth-order, first-order, and second-order truncated three-simplex lattices.

quantum search on truncated simplex lattices of any order is still missing. Quantum search on truncated simplex lattices of higher than first order has never been solved. Furthermore, an optimal search has never been achieved in truncated simplex lattices of higher than zeroth order.

We mount this challenge in this paper. By numerically calculating the spectrum of the Hamiltonian, we present a comprehensive study of quantum search on truncated simplex lattices of any order exploiting a multistage search process and numerically give the required number of stages, the critical jumping rate, and the run time for the multistage process. Furthermore, we numerically show that when we increase the weights of some edges, the two-stage search process can be merged into one stage for first-order truncated simplex lattices, which provides a substantial speedup and achieves an optimal run time proportional to the square root of the number of vertices. Thus, an optimal search on the first-order truncated simplex lattice is achieved by our scheme. This paper also serves as another important example of quantum search via CTQW on hierarchical graphs, exhibiting the requirement for a multistage search process and merging of stages which we proposed to be the possible common properties of quantum search on hierarchical graphs in Ref. [38].

The structure of the paper is as follows. We discuss any-order truncated simplex lattices and propose a multistage search process in Sec. II. Next, we discuss the merging of stages and optimal search algorithm in Sec. III. We then discuss the robustness of our results in Sec. IV and, finally, give our discussion and conclusion in Sec. V.

II. MULTISTAGE QUANTUM SEARCH ON TRUNCATED SIMPLEX LATTICES

We first briefly introduce the structure of truncated M-simplex lattices on which the quantum search is performed in our discussion, following the notations in [1]. The zeroth-order truncated M-simplex lattice is a complete graph with $(M+1)$ vertices. To get an $(r+1)$th-order truncated M-simplex lattice, we replace every vertex in the rth-order truncated M-simplex lattice with a complete graph of M vertices each of which is connected to a different cluster. Therefore, the number of vertices in the rth-order truncated M-simplex lattice is $N=(M+1)M^r$. Several examples of truncated M-simplex lattices are shown in Fig. 1. Existing discussion about quantum search on the truncated M-simplex lattice is limited to the zeroth and first orders [9,10,12,13,37]. Especially, Ref. [10] gives a novel two-stage search algorithm on the first-order M-simplex lattice. We would like to explore

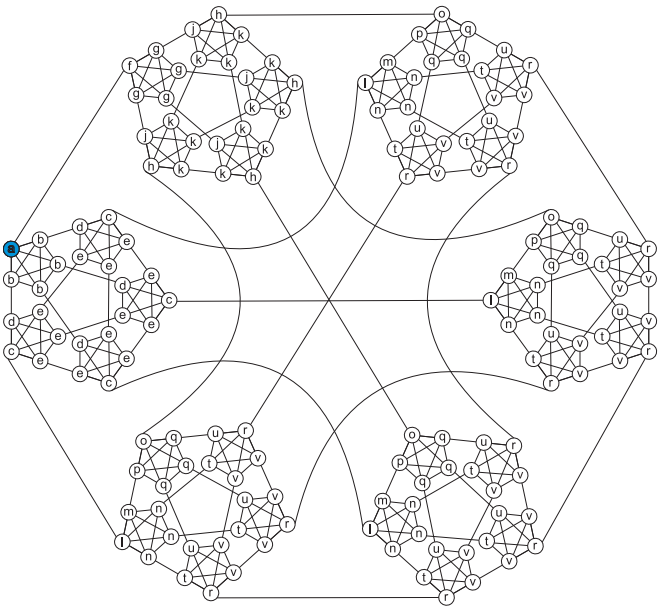

FIG. 2. Second-order truncated five-simplex lattice with identically evolving vertices labeled with the same letter. The blue vertex is the marked vertex a.

the quantum search via CTQW on any-order truncated M-simplex lattices in this section. It turns out that a multistage searching scheme is required to achieve a success probability close to 100%.

As the first example to illustrate our quantum search scheme on this type of graph, we focus on the second-order truncated M-simplex lattice. The case for $M=5$ is explicitly shown in Fig. 2 for illustration, but M should be large enough to get a success probability close to 100% in our quantum search scheme. The results below hold for any M which is large enough.

Following Childs and Goldstone [9], the basis states $\{|1\rangle, |2\rangle, \ldots, |N\rangle\}$ of an N-dimensional Hilbert space corresponds to the N vertices of a given graph. Since we have no information on the position of the marked state, the initial state is chosen as the equal superposition of all vertices of the graph $|s\rangle = \frac{1}{\sqrt{N}}\sum_{i=1}^{N}|i\rangle$. After the evolution of the system, we expect to accumulate probability amplitude at the marked vertex a. The Hamiltonian is chosen as

$$H = -\gamma L - |a\rangle\langle a|, \tag{1}$$

where γ is the jumping rate, $|a\rangle\langle a|$ is a quantum oracle, $L=A-D$ is the graph Laplacian, A is the adjacency matrix of the graph, whose element A_{ij} indicates the weight of the edge between vertex i and vertex j, and D is a diagonal matrix whose ith diagonal term is the total weight of edges connected to vertex i. D can be dropped by rezeroing the ground-state energy for truncated M-simplex lattices since they are regular graphs, i.e., each vertex has the same number of neighbors. For convenience, we choose a dimensionless Hamiltonian H and time.

The marked vertex can have two nonequivalent positions, either connected to an outside vertex or connected only to vertices in the same level. We discuss the former one first, and

suppose the marked vertex is a. We can group together the nonmarked vertices which evolve identically to simplify the calculation by working in an invariant subspace of the Hamiltonian. From the symmetry of the graph, we find that there are 20 different types of vertices, labeled with 20 different letters in Fig. 2. The labels run from a to v except for the letters i and s, with i reserved for the index in summation and s reserved for the initial symmetric state. Hence, the dimension of the invariant subspace is 20, which is independent of M. Each basis state of the invariant subspace corresponds to an equal superposition of the original vertex states in a particular type. Let $|x\rangle$ denote the normalized basis state corresponding to the x type of vertices. For example, $|b\rangle = \frac{1}{\sqrt{M-1}}\sum_{i\in b}|i\rangle$, $|e\rangle = \frac{1}{\sqrt{(M-2)(M-1)}}\sum_{i\in e}|i\rangle$, $|v\rangle = \frac{1}{\sqrt{(M-3)(M-2)(M-1)}}\sum_{i\in v}|i\rangle$, and so on. The Hamiltonian $H = -\gamma A - |a\rangle\langle a|$ can be expressed in the invariant subspace. The adjacency matrix A in this subspace is shown in Table I in Appendix A.

We now describe our three-stage searching scheme on a second-order truncated M-simplex lattice. Following Refs. [9] and [10], to see why a multistage searching process is required, we should first analyze the squared overlaps between eigenstates $|\psi_0\rangle, |\psi_1\rangle, \ldots, |\psi_n\rangle$, where $|\psi_i\rangle$ is the ith eigenstate of Hamiltonian H, and the basis states or the initial state $|s\rangle$, which is shown in Fig. 3. The obvious crossing points at $\gamma = 1/M$, $2/M$, and $3/M$, respectively, in the figure indicate that the eigenstates are dominated by more than one basis state. These values of γ where crossings occur are the critical jumping rates. To transfer the probability between vertices, these crossings are necessary. Because when γ deviates from the crossing points, the basis states are almost eigenstates and the amplitude of each basis state will only gain a phase during the evolution of the system, while at these crossing points, the probability amplitude will oscillate between two basis states. For example, at $\gamma = 3/M$ we obtain numerically two of the eigenstates of H as $|\psi_{0,1}\rangle \approx (|s\rangle \pm |e\rangle)/\sqrt{2}$. The deviation of eigenstates from this relation is shown in Fig. 4. Therefore, when $\gamma = 3/M$ we have $|s\rangle \approx (|\psi_0\rangle + |\psi_1\rangle)/\sqrt{2}$ and

$$|\psi(t)\rangle = e^{-iHt}|s\rangle \approx \frac{1}{\sqrt{2}}(e^{-iE_0t}|\psi_0\rangle + e^{-iE_1t}|\psi_1\rangle), \qquad (2)$$

with the state of the system oscillating between $|s\rangle$ and $|e\rangle$, i.e., $|\langle e|\psi(t)\rangle|^2 \approx \frac{1}{2}(1-\cos\Delta E_{10}t)$, $|\langle s|\psi(t)\rangle|^2 \approx \frac{1}{2}(1+\cos\Delta E_{10}t)$. The oscillation period is given by the energy gap $\Delta E_{10} = E_1 - E_0$. After time $t = \pi/\Delta E_{10}$, almost all of the probability amplitude is accumulated in basis state $|e\rangle$. Exploiting this oscillation, we can transfer the probability amplitude from the initial state $|s\rangle$ to state $|e\rangle$ at $\gamma = 3/M$ with time $t = \pi/(E_1 - E_0)$, from state $|e\rangle$ to state $|b\rangle$ at $\gamma = 2/M$ with time $t = \pi/(E_3 - E_0)$, and from state $|b\rangle$ to state $|a\rangle$ at $\gamma = 1/M$ with time $t = \pi/(E_7 - E_0)$. After most of the probability amplitude is accumulated at the marked vertex a, we only need a simple vertex measurement to locate it. Thus, a three-stage searching process is required for our purpose. This actually also gives strong constraints on the choice of initial states. The overlap of the initial states should be dominated by at least two eigenstates at some values of the jumping rate γ so that the probability amplitude can be transferred through the oscillation between two basis states. Combined with the fact that we have no information about the initial states, $|s\rangle$ is a proper choice as the initial state.

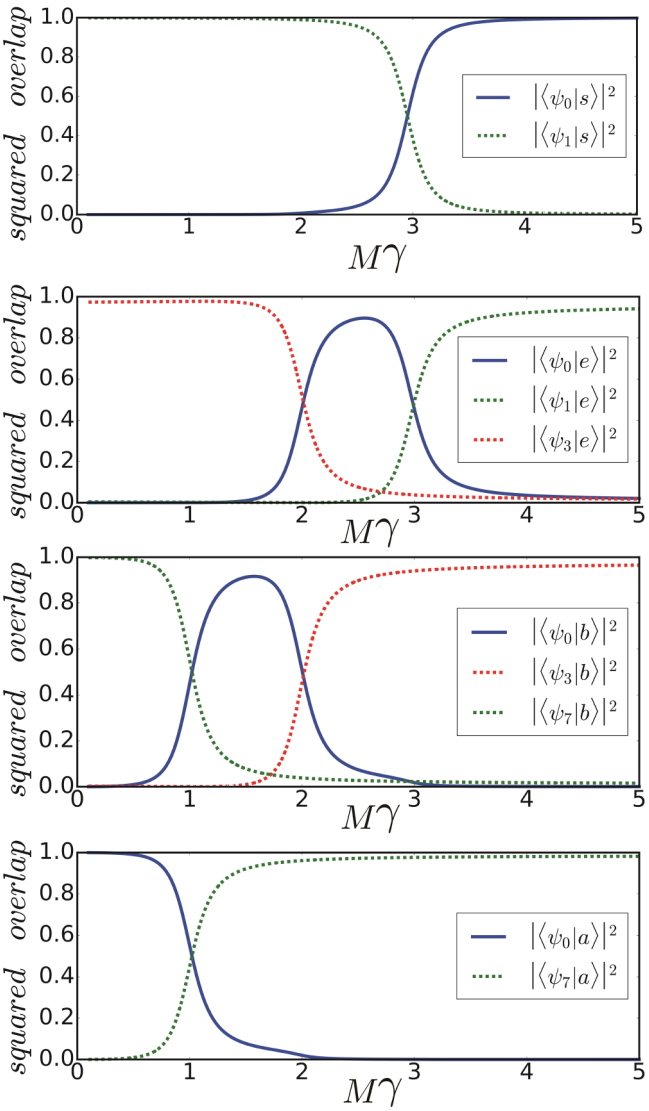

FIG. 3. Squared overlaps of basis states with the eigenstates of H on a second-order truncated M-simplex lattice. $|\psi_i\rangle$ is the ith eigenstate of the Hamiltonian H. $M = 100$.

The energy gap is derived numerically and the searching time in each stage is chosen accordingly. For the first stage, with $\gamma = 3/M$, we find that $E_1 - E_0 = 6M^{-\frac{5}{2}} - 14.25M^{-\frac{7}{2}} + o(M^{-\frac{7}{2}})$, and we choose the searching time in this stage as $T_1 = \pi/(E_1 - E_0) = \pi M^{\frac{5}{2}}/6$. For the second stage, with $\gamma = 2/M$, we find $E_3 - E_0 = 4M^{-\frac{3}{2}} - 11.5M^{-\frac{5}{2}} + o(M^{-\frac{5}{2}})$, and we choose the searching time in this stage as $T_2 = \pi M^{\frac{3}{2}}/4$. For the third stage, with $\gamma = 1/M$, we find $E_7 - E_0 = 2M^{-\frac{1}{2}} + 0M^{-\frac{3}{2}} + o(M^{-\frac{3}{2}})$, and we choose the searching time in this stage as $T_3 = \pi M^{\frac{1}{2}}/2$. When M is large enough (for example, $M = 1000$), the success probability $|\langle a|\psi(t = T_1 + T_2 + T_3)\rangle|^2$ is larger than 99%. The influence of M on the success probability is shown in Fig. 5. The dominant term of the run time in the search process is $t \propto M^{\frac{5}{2}} \propto N^{\frac{5}{6}}$.

So far, we have considered just one possible position of the marked vertex and have not discussed the other inequivalent

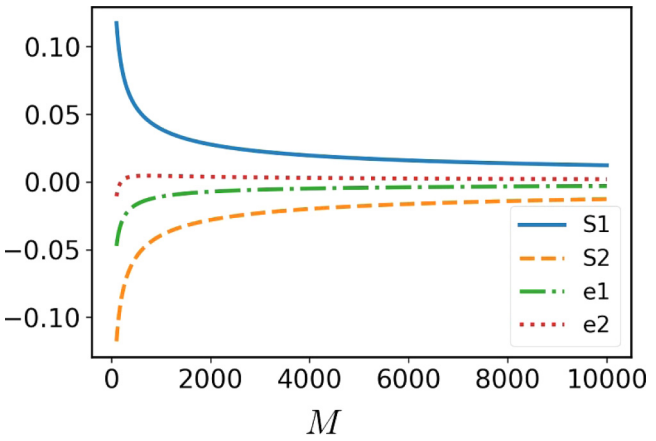

FIG. 4. Deviation from the approximated relation $|\psi_{0,1}\rangle \approx (|s\rangle \pm |e\rangle)/\sqrt{2}$. The line labeled 'S1' is $|\langle s|\psi_0\rangle|^2 - 0.5$, the line labeled 'S2' is $|\langle s|\psi_1\rangle|^2 - 0.5$, the line labeled 'e1' is $|\langle e|\psi_0\rangle|^2 - 0.5$, and the line labeled 'e2' is $|\langle e|\psi_1\rangle|^2 - 0.5$.

case where the marked vertex is only connected to the vertices in the same level (for example, one of the vertices labeled b is the marked one). For the other case (for the second-order lattice, there are only two possible inequivalent positions), even though the dimension of the invariant subspace is different, we find that the number of stages, the critical jumping rate, and the proper searching time in each stage are almost the same. We have verified numerically that the three-stage algorithm with the same jumping rate and searching time in each stage achieves a success probability higher than 99%, when M is large enough (for example, $M = 1000$).

We have pointed out the necessity for a three-stage searching process on a second-order truncated M-simplex lattice from the perspective of crossing points in the overlaps of basis states with eigenstates in Fig. 3. We want to provide a more intuitive point of view from the flux of probability amplitude in each stage. In the first stage, the probability amplitude will flow from $|s\rangle$ to $|e\rangle$. Since $|s\rangle \approx |v\rangle$, we can regard this as the flow from $|v\rangle$ to $|e\rangle$, i.e., the probability amplitude will flow from the outermost complete graph to the interior complete graph. In the second stage, the probability amplitude will flow

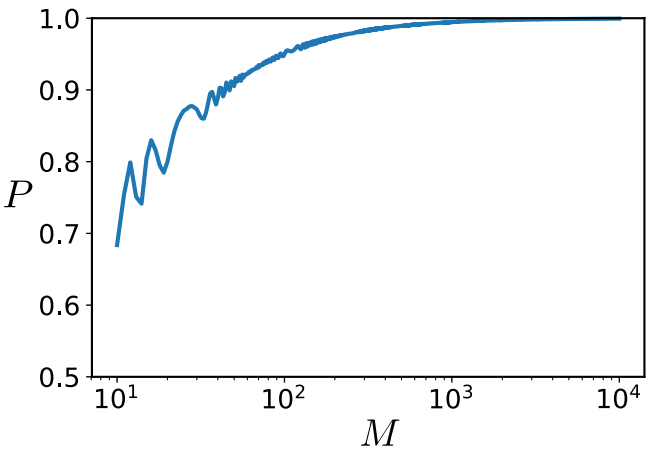

FIG. 5. Success probability versus M on a second-order truncated M-simplex lattice.

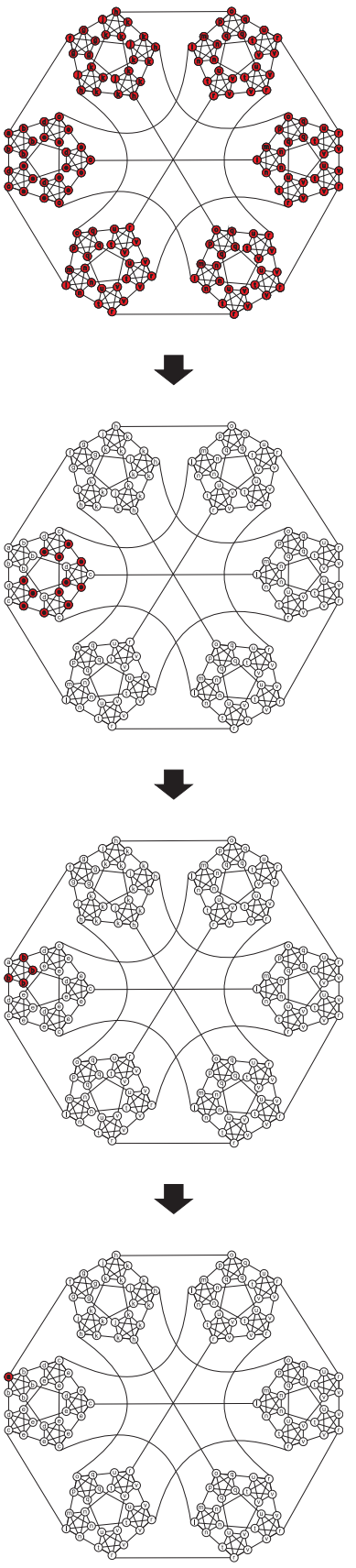

FIG. 6. Evolution of the probability distribution on a second-order truncated five-simplex lattice.

from $|e\rangle$ to $|b\rangle$, hence closer to the interior. In the third stage, the flow occurs in the innermost complete graph from $|b\rangle$ to $|a\rangle$. Probability flow into the interior structure has been pointed out in first-order truncated M-simplex lattices [12]. Our results show that this is true in higher-order cases. We show the distribution of the dominant part of the probability amplitude at the end of each stage in Fig. 6. The multistage probability amplitude flow is closely related to the hierarchical structure of graphs, which implies a multistage searching process.

Having revealed that the quantum search scheme on the second-order truncated M-simplex lattice shows regular rules for the choice of jumping rate and run time at each stage, one might expect similar rules for quantum search on rth-order truncated M-simplex lattices ($r = 0, 1, 2, 3, \dots$) in general. The procedure to express the Hamiltonian of any-order truncated M-simplex lattices in the invariant subspace is similar. We have further explicitly calculated up to fifth-order truncated M-simplex lattices as explained in Appendix B and obtained the following results. For an rth-order truncated M-simplex lattice, the search process requires $(r+1)$ stages with different jumping rates $\gamma = \frac{r+1}{M}, \frac{r}{M}, \dots, \frac{2}{M}, \frac{1}{M}$; the run time in each stage is $t \propto M^{\frac{2r+1}{2}}, M^{\frac{2r-1}{2}}, \dots, M^{\frac{3}{2}}, M^{\frac{1}{2}}$ (i.e., $t \propto N^{\frac{2r+1}{2r+2}}, N^{\frac{2r-1}{2r+2}}, \dots, N^{\frac{3}{2r+2}}, N^{\frac{1}{2r+2}}$), respectively, and the dominant term of time consumed in the search process is therefore $t \propto M^{\frac{2r+1}{2}} \propto N^{\frac{2r+1}{2r+2}}$. The argument about the necessity for a multistage searching process can also be applied to rth-order truncated M-simplex lattices in general.

Quantum search on a zeroth-order truncated M-simplex lattice (complete graph) and a first-order truncated M-simplex lattice was also discussed in Ref. [9] and Ref. [10], respectively. Here we have discussed any order of truncated M-simplex lattice, and our numerical results coincide with the previous references for the two special situations which have been proved carefully. The equivalent continuous-time analogy of Grover's algorithm can be interpreted as quantum search using a continuous-time quantum walk on a zeroth-order truncated M-simplex lattice, and it can provide a full $\sqrt{N}$ speedup [9,39], which is also consistent with our results.

Our results show that a higher order of truncated M-simplex lattice indicates a slower search compared to Grover's algorithm since $t \propto M^{\frac{2r+1}{2}} \propto N^{\frac{2r+1}{2r+2}}$. This can be understood because a higher order corresponds to more levels in the graph, which will introduce more restrictions on the flow of probability. Therefore, for truncated M-simplex lattices, order is an important indicator of the graph complexity and the speed of quantum search. Whether this indicator could be generalized to other graphs is an interesting topic for further discussion.

An interesting observation is the shift of the dominant component of the ground state $|\psi_0\rangle$ of the Hamiltonian when γ is changing around the critical jumping rate γ_c. For quantum search on a second-order truncated M-simplex lattice, when γ changes from larger than $3/M$ to smaller than $1/M$, $|\psi_0\rangle$ is dominated by $|s\rangle$, $|e\rangle$, $|b\rangle$, and $|a\rangle$ in turn when γ is not too close to $1/M$, $2/M$, and $3/M$. Three shifts and an exactly equal number of stages in the search process suggest to us that the number of these shifts might indicate the number of stages in general.

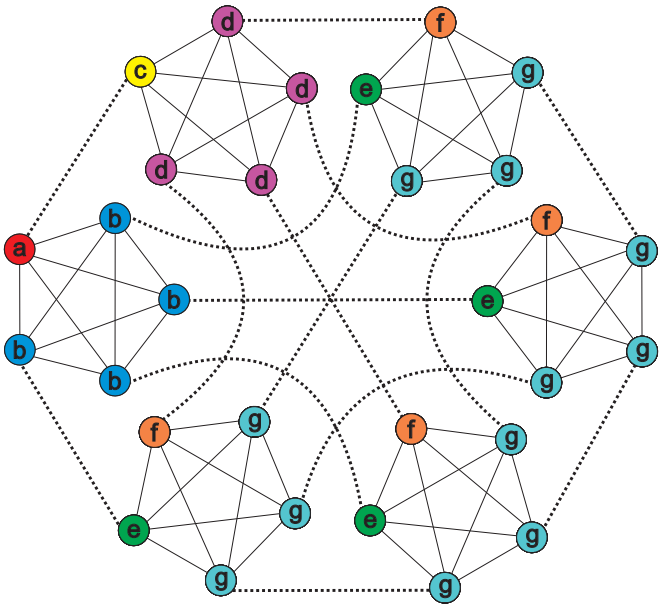

FIG. 7. A truncated first-order five-simplex lattice. Solid edges have weight 1 and dotted edges have weight ω.

III. MERGING OF STAGES IN QUANTUM SEARCH

It has been argued that although the first-order truncated simplex lattice is well connected, it does not support an optimal quantum search [10]. We have seen that for higher-order truncated M-simplex lattices, the multistage searching process required to achieve a high success probability becomes even slower. However, in this section we show that we can accelerate this process. It is shown in Ref. [12] that a faster quantum search using CTQW can be achieved on the first-order truncated M-simplex lattice by changing the weight of edges, but the optimal search speed is not achieved, as only the case with $\omega = o(\sqrt{M})$ is considered. As suggested by Ref. [12], we further show that for the first-order truncated M-simplex lattice higher edge weights can lead to the merging of stages in the sense that only one stage is required to achieve a high success probability, combined with the realization of the optimal search speed.

The case of first-order truncated M-simplex lattices with $M = 5$ is shown in Fig. 7, but the discussion below holds for any large enough M. We set the weight of dotted edges as ω. The Hamiltonian can be written in the seven-dimensional invariant subspace as

$$H = -\gamma \begin{bmatrix} \frac{1}{\gamma} & \sqrt{M_1} & \omega & 0 & 0 & 0 & 0 \\ \sqrt{M_1} & M_2 & 0 & 0 & \omega & 0 & 0 \\ \omega & 0 & 0 & \sqrt{M_1} & 0 & 0 & 0 \\ 0 & 0 & \sqrt{M_1} & M_2 & 0 & \omega & 0 \\ 0 & \omega & 0 & 0 & 0 & 1 & \sqrt{M_2} \\ 0 & 0 & 0 & \omega & 1 & 0 & \sqrt{M_2} \\ 0 & 0 & 0 & 0 & \sqrt{M_2} & \sqrt{M_2} & M_3 + \omega \end{bmatrix},$$

where $M_l = M - l$. Numerically, we find that when ω is larger than roughly $M^{\frac{3}{4}}$, the two stages are merged into one.

From the perturbation theory perspective, we can discuss the quantum search using CTQW analytically [40]. The basic idea is to separate the Hamiltonian into leading and

higher-order terms, then calculate the eigenstates of leading terms of the Hamiltonian. Let two eigenstates of the leading terms of the Hamiltonian be degenerate by controlling γ and then consider the higher-order Hamiltonian to split degeneracy and find the energy gap. Assuming that ω scales over M more rapidly than $M^{\frac{3}{4}}$, and dropping all terms of the Hamiltonian which scale less than $M^{\frac{3}{4}}$, we have the leading terms of the Hamiltonian

$$H^{(0)} = -\gamma \begin{bmatrix} \frac{1}{\gamma} & 0 & \omega & 0 & 0 & 0 & 0 \\ 0 & M & 0 & 0 & \omega & 0 & 0 \\ \omega & 0 & 0 & 0 & 0 & 0 & 0 \\ 0 & 0 & 0 & M & 0 & \omega & 0 \\ 0 & \omega & 0 & 0 & 0 & 0 & 0 \\ 0 & 0 & 0 & \omega & 0 & 0 & 0 \\ 0 & 0 & 0 & 0 & 0 & 0 & M+\omega \end{bmatrix}.$$

We know that $|s\rangle = \frac{1}{\sqrt{N}} \sum_{i=1}^{N} |i\rangle \approx |g\rangle$, and we want the probability to be accumulated at the marked vertex a. The eigenstates that need to be degenerate are $|g\rangle$ with energy $E_g = -\gamma M - \gamma\omega$ and $|u\rangle = -\gamma\omega/(-\frac{1}{2}\sqrt{4\gamma^2\omega^2+1} + \frac{1}{2})|a\rangle + |c\rangle$ with energy $E_u = -\frac{1}{2} - \frac{1}{2}\sqrt{4\gamma^2\omega^2+1}$. Making the two eigenstates degenerate, i.e., $E_g = E_u$, we obtain the critical jumping rate: $\gamma_c = \frac{1+\omega/M}{1+2\omega/M}\frac{1}{M}$.

For the special case where $\omega = M$, we have $\gamma_c = \frac{2}{3}\frac{1}{M}$. Following Ref. [9], we plot the overlaps between the basis states and the eigenstates explicitly in Fig. 8. We can observe an obvious crossing point at about $\gamma M = 2/3$ as predicted previously. Numerically, we find that $E_1 - E_0 = \frac{8}{3}M^{-1} + o(M^{-1})$. Choosing the searching time as $t = \frac{3}{8}\pi M$, we find that the success probability is roughly 36%. But one could actually read from Fig. 8 that the probability which can oscillate between $|s\rangle$ and $|a\rangle$ is roughly 75%. So the higher-order terms ignored in the discussion using perturbation theory [40] are important in this problem. The success probability could be higher with a slightly different γ. We thus fine-tune γ to find a higher achievable success probability. Numerically, we find that when $\gamma = \frac{2}{3}\frac{1}{M} + \frac{2}{M^2}$, $E_1 - E_0 = 1.83M^{-1} + o(M^{-1})$, choosing the searching time as $t = \pi M/1.83$, the success probability is roughly 75%. Fixing the γ and the searching time, the variation of the success probability versus M is shown in Fig. 9. This might inspire us to further develop the method in Ref. [40] by treating the high-order terms more carefully in order to find a more proper γ; this is, however, beyond the purpose of this paper.

One might worry whether the numerical results for the energy gap deviate slightly from the scaling $E_1 - E_0 \propto M^{-1}$, which is not captured by the numerical calculation. For example, $E_1 - E_0 \propto M^{-1-\epsilon}$ for some small ϵ. However, we want to point out that the numerical result for the energy gap is only used to design the search scheme. After the scheme is designed, we keep the searching strategy (including the searching time and critical jumping rate) fixed for any number of vertices. Whether the energy gap is properly calculated should be tested by the scheme's success probability for different numbers of vertices, which are exactly the results shown in Fig. 9. Since the success probability of the scheme tends to a large constant value as M increases, all the higher-order terms of the energy gap we dropped should be negligible. This argument is also true for the multistage search scheme discussed in the previous section.

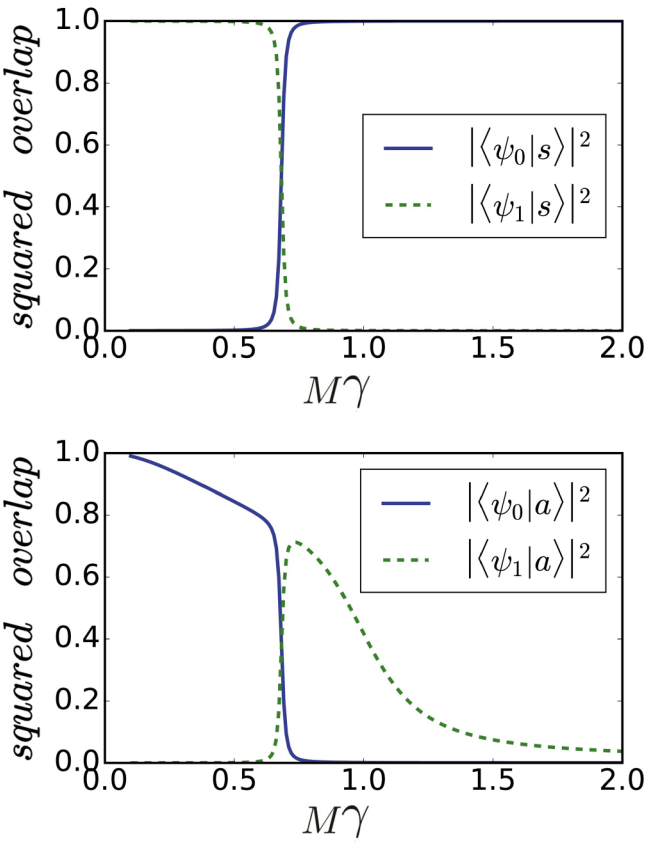

FIG. 8. Overlaps between basis states and eigenstates of the Hamiltonian for a weighted first-order truncated M-simplex lattice when $\omega = M = 100$.

Here we numerically demonstrate the optimal run time on a first-order truncated simplex lattice. However, we should note that upon increasing the weight of edges, the connectivity does increase. An equally weighted first-order truncated simplex lattice has an algebraic connectivity of 1 and a normalized algebraic connectivity of $\Theta(1/\sqrt{N})$. A weighted first-order truncated simplex lattice with $\omega = M$ has an algebraic con-

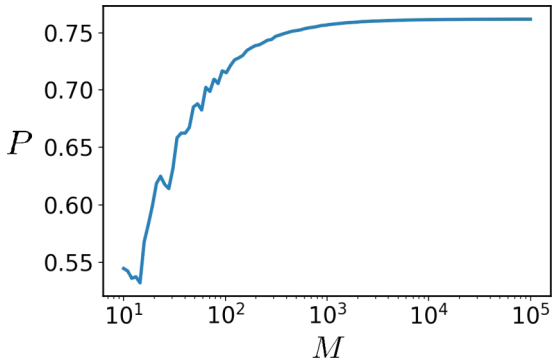

FIG. 9. Success probability versus M on a weighted first-order truncated M-simplex lattice where $\omega = M$, $\gamma = \frac{2}{3}\frac{1}{M} + \frac{2}{M^2}$, and the run time is chosen as $t = \pi M/1.83$.

nectivity of roughly $0.38\sqrt{N}$ and a normalized algebraic connectivity of roughly 0.38.

We want to point out that when a large enough gap exists between the largest two eigenvalues of the graph Laplacian L, the optimal quantum search should be able to be achieved according to a sufficient condition proposed in Ref. [30]. In Sec. II, the gap between the largest two eigenvalues of the Laplacian of the truncated M-simplex lattice is not large enough. An optimal search is not achieved. In Sec. III, with adjusted edge weights, the Laplacian of the first-order truncated M-simplex lattice when $\omega = M$ does have a sufficiently large gap between the largest two eigenvalues of the Laplacian, and an optimal quantum search with run time $O(\sqrt{N})$ is indeed achieved. These conclusions are consistent with the condition.

Furthermore, from our discussion it seems that increasing the weights of edges between poorly connected parts of the graph may provide a possible way to increase the gap between the largest two eigenvalues of the graph Laplacian L. This observation may be useful for other types of graphs as well.

IV. ROBUSTNESS OF THE QUANTUM SEARCH

In this section, we discuss how noise affects the quantum search on a truncated M-simplex lattice. For simplicity, the noise is introduced, as the weight of some edges in the graph varies from its ideal value, and we only consider the case where M is large enough. We directly apply the algorithms proposed for unweighted and weighted graphs in the previous sections to the corresponding graphs with varied weights (i.e., in the presence of noise), and we calculate the success probability and show how it is affected by the noise. In other words, we choose the same number of stages, jumping rate, and run time of each stage as proposed before and show how the presence of noise will decrease the success probability. The following situations are considered.

(i) We first consider a two-stage quantum search on an unweighted first-order truncated simplex lattice, and we find that a small variation of the weight of a single edge between two vertices in the same group (for example, in group b) does not affect the two-stage search process considerably. This can be easily observed when we find the corresponding matrix of the Hamiltonian in the invariant subspace. Assume that the weight of the edge between two vertices b_1 and b_2 in group b is changed to be an arbitrary value ω. Now the state is still evolving in a subspace which is spanned by $\{|a\rangle, |b'\rangle, |b''\rangle, |c\rangle, |d\rangle, |e\rangle, |f\rangle, |g\rangle\}$, where $|b'\rangle = \frac{1}{\sqrt{2}}(|b_1\rangle + |b_2\rangle)$ and $|b''\rangle = \frac{1}{\sqrt{M-3}}\sum_{i\neq 1,2, i\in b}|b_i\rangle$. The only matrix of elements of the effective Hamiltonian affected by the perturbation is $\langle b'|H|b'\rangle = -\gamma\langle b'|L|b'\rangle = \gamma[-M-(\omega-1)+\omega] = \gamma(-M+1)$, which is actually independent of ω. This means that any perturbation on a single edge between the vertices in the same group will not affect the search process. [But the further perturbation on edges between vertices in different groups could affect the search process as discussed in paragraph (ii).] This means that if we have groups with a large number of vertices, which require more symmetries of the graphs, there is more room to tolerate noise on the edges. The symmetries of the graphs are only used to reduce the matrix size of the Hamiltonian in all previous discussion. But in this discussion, we suggest that

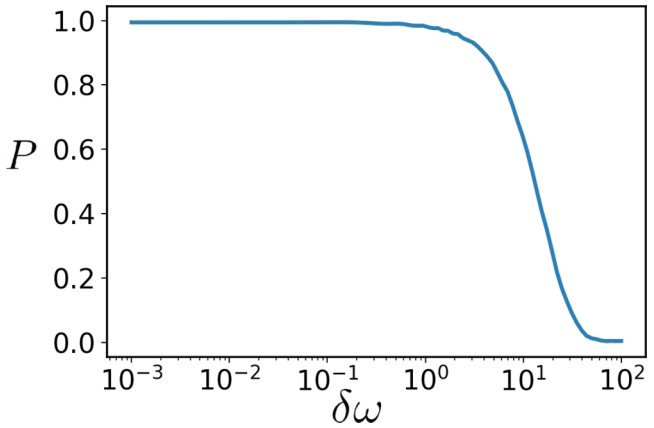

FIG. 10. Success probability versus a variation $\delta\omega$ of the weight of a single edge between two vertices in different groups for a first-order truncated M-simplex lattice with $M = 100$.

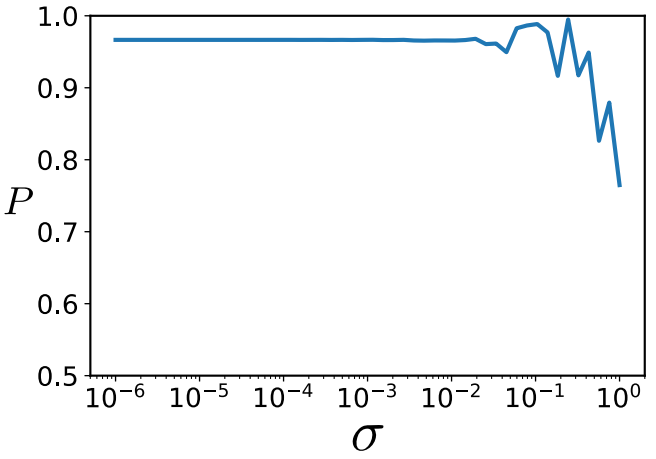

FIG. 11. Influence of Gaussian noise on the success probability for a first-order truncated M-simplex lattice with $M = 50$.

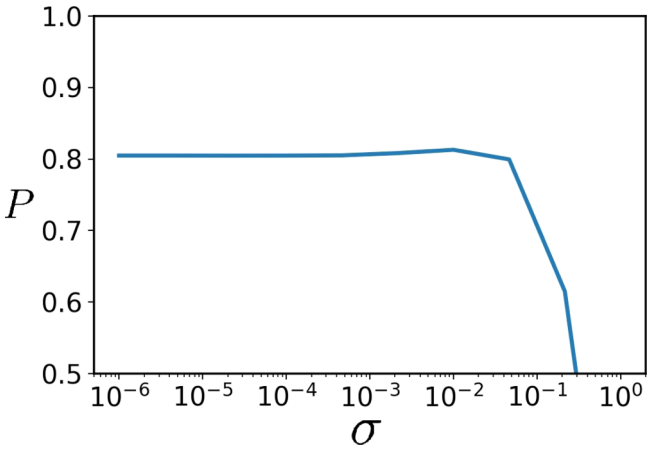

FIG. 12. Influence of Gaussian noise on the success probability for a second-order truncated M-simplex lattice with $M = 15$.

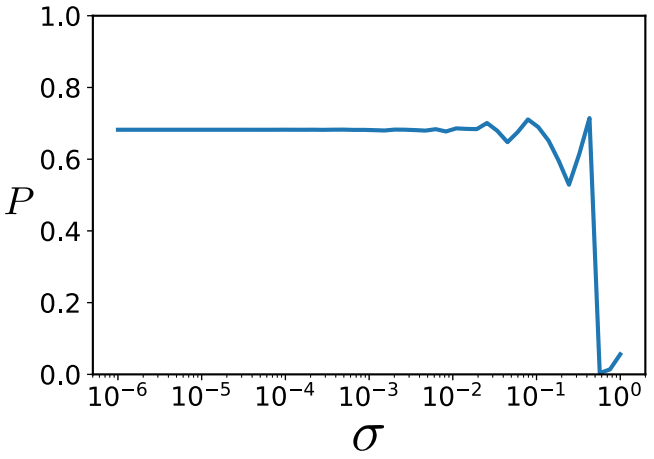

FIG. 13. Influence of Gaussian noise on the success probability for a weighted first-order truncated M-simplex lattice with $M = \omega = 50$.

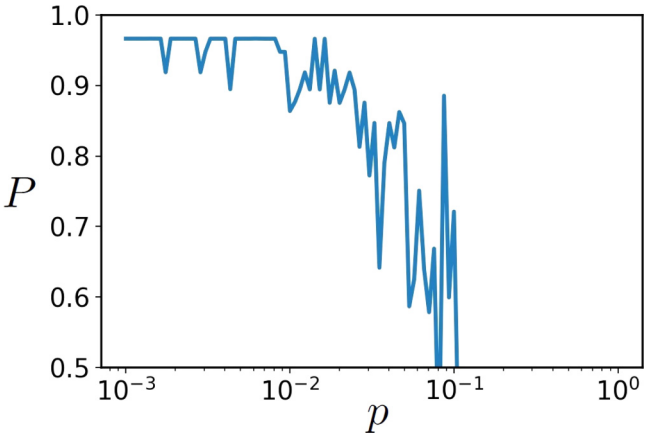

FIG. 14. Influence on the success probability of modifying the edge weight to be $\omega = 2$ with probability p for a first-order truncated M-simplex lattice with $M = 50$.

the symmetries of the graphs might play a very important role when we include the error in the discussion.

(ii) On an unweighted first-order truncated simplex lattice with the unperturbed weight of all edges being 1, an increase in the weight of a single edge $\delta\omega$ between two vertices (with one from group a and the other from group b) up to the amount scaling more slowly than roughly $M^{\frac{1}{2}}$ does not affect the two-stage search considerably as shown in Fig. 10. When the variation of this weight $\delta\omega$ is scaling more rapidly than $M^{\frac{1}{2}}$, we observe a considerable decrease in the success probability.

(iii) We add Gaussian noise to every edge weight of an unweighted first-order truncated M-simplex lattice; the influence of noise on the success probability is shown in Fig. 11. We find that the success probability does not change much when the standard deviation σ is smaller than 10^{-2}.

(iv) We add Gaussian noise to every edge weight of an unweighted second-order truncated M-simplex lattice; the influence of noise on the success probability is shown in Fig. 12. Assuming that the marked vertex is in the outermost layer of the graph as shown in Fig. 2, we find that the success probability does not change much when the standard deviation σ is smaller than 10^{-2}.

(v) Starting from an ideal weighted first-order truncated M-simplex lattice as shown in Fig. 7, with dotted edges having weight M, we add Gaussian noise to every edge weight; the influence of noise on the success probability is shown in Fig. 13. When the standard deviation σ is smaller than 10^{-2}, no influence is observed.

(vi) On an unweighted first-order truncated simplex lattice, assume that each edge weight is modified to be $\omega = 2$ with probability p. We show how the probability of modifying the weight of edges affects the success probability in Fig. 14.

TABLE I. Adjacency matrix A of a second-order truncated M-simplex lattice in the invariant subspace, where $M_l = M - l$.

0	$\sqrt{M_1}$	0	0	0	1	0	0	0	0	0	0	0	0	0	0	0	0	0	0
$\sqrt{M_1}$	M_2	0	1	0	0	0	0	0	0	0	0	0	0	0	0	0	0	0	0
0	0	0	1	$\sqrt{M_2}$	0	0	0	0	0	1	0	0	0	0	0	0	0	0	0
0	1	1	0	$\sqrt{M_2}$	0	0	0	0	0	0	0	0	0	0	0	0	0	0	0
0	0	$\sqrt{M_2}$	$\sqrt{M_2}$	M_2	0	0	0	0	0	0	0	0	0	0	0	0	0	0	0
1	0	0	0	0	0	$\sqrt{M_1}$	0	0	0	0	0	0	0	0	0	0	0	0	0
0	0	0	0	0	$\sqrt{M_1}$	M_2	0	1	0	0	0	0	0	0	0	0	0	0	0
0	0	0	0	0	0	0	0	1	$\sqrt{M_2}$	0	0	0	1	0	0	0	0	0	0
0	0	0	0	0	0	1	1	0	$\sqrt{M_2}$	0	0	0	0	0	0	0	0	0	0
0	0	0	0	0	0	0	$\sqrt{M_2}$	$\sqrt{M_2}$	M_2	0	0	0	0	0	0	0	0	0	0
0	0	1	0	0	0	0	0	0	0	0	1	$\sqrt{M_2}$	0	0	0	0	0	0	0
0	0	0	0	0	0	0	0	0	0	1	0	$\sqrt{M_2}$	0	1	0	0	0	0	0
0	0	0	0	0	0	0	0	0	0	$\sqrt{M_2}$	$\sqrt{M_2}$	M_3	0	0	0	0	1	0	0
0	0	0	0	0	0	0	1	0	0	0	0	0	0	1	$\sqrt{M_2}$	0	0	0	0
0	0	0	0	0	0	0	0	0	0	0	1	0	1	0	$\sqrt{M_2}$	0	0	0	0
0	0	0	0	0	0	0	0	0	0	0	0	0	$\sqrt{M_2}$	$\sqrt{M_2}$	M_3	0	0	1	0
0	0	0	0	0	0	0	0	0	0	0	0	0	0	0	0	1	1	1	$\sqrt{M_3}$
0	0	0	0	0	0	0	0	0	0	0	0	1	0	0	0	1	0	1	$\sqrt{M_3}$
0	0	0	0	0	0	0	0	0	0	0	0	0	0	0	1	1	1	0	$\sqrt{M_3}$
0	0	0	0	0	0	0	0	0	0	0	0	0	0	0	0	$\sqrt{M_3}$	$\sqrt{M_3}$	$\sqrt{M_3}$	M_3

When $p > 10^{-2}$, the success probability is obviously suppressed.

Therefore, our quantum algorithms are quite robust against the presence of noise that causes a small variation of the weight of some edges. However, a large variation in edge weight could destroy the search process.

V. CONCLUSION AND DISCUSSION

In summary, we have studied multistage quantum search on truncated simplex lattices of up to fifth order when the edges are equally weighted. The search process requires $r+1$ stages and the dominant term of the proper searching time in the search process is $\Theta(N^{(2r+1)/(2r+2)})$. We have studied quantum search on the first-order truncated simplex lattice when the edge weight is adjustable. We show that the different stages can be merged into a single stage, leading to a substantial speedup and realization of an optimal search with run time $\Theta(\sqrt{N})$. We have checked the quantum search on first-order and second-order truncated simplex lattices to show that the schemes are quite robust under several types of small noise. We conjecture that these conclusions are generally true for truncated simplex lattices of any order.

The merging of stages is achieved by adjusting the edge weights of the graph, which might cause more energy usage. The operator norm of the Hamiltonian indicates the energy consumed in the search [12]. For the first-order truncated M-simplex lattice, the operator norm is $\gamma(M+\omega-1)$. When one sets $\omega = M$ to merge the two stages into a single one, more energy is consumed, but it is of the same magnitude. So the optimal search is not simply achieved by adding more energy into the system. Actually, one can prove that the average energy is a constant regardless of whether the edges are weighted, $\langle E(t)\rangle = \langle\psi(t)|H|\psi(t)\rangle = -\langle s|\gamma L|s\rangle - \langle s|a\rangle\langle a|s\rangle = -1/N$. Whether some alternative modification of the structure or other methods could cause this merging also deserves further discussion since this could provide a faster and easier search.

The quantum search schemes for truncated simplex lattices in this paper, together with those for balanced trees in Ref. [38], clearly indicate that quantum search via CTQW on hierarchical graphs, in general, requires a multistage scheme when the edge weights are not adjustable, but an optimal single-stage scheme can also be designed when the edge weights are controllable.

ACKNOWLEDGMENTS

We thank Andrew M. Childs, Yunchu Wang, and Kejie Fang for valuable discussions. This work was supported by the National Key R&D Program of China (Grants No. 2017YFA0303703 and No. 2016YFA0301801) and the National Natural Science Foundation of China (Grant No. 11475084).

APPENDIX A: THE ADJACENCY MATRIX IN THE SUBSPACE

The adjacency matrix A of the second-order truncated M-simplex lattice in the invariant subspace is given in Table I.

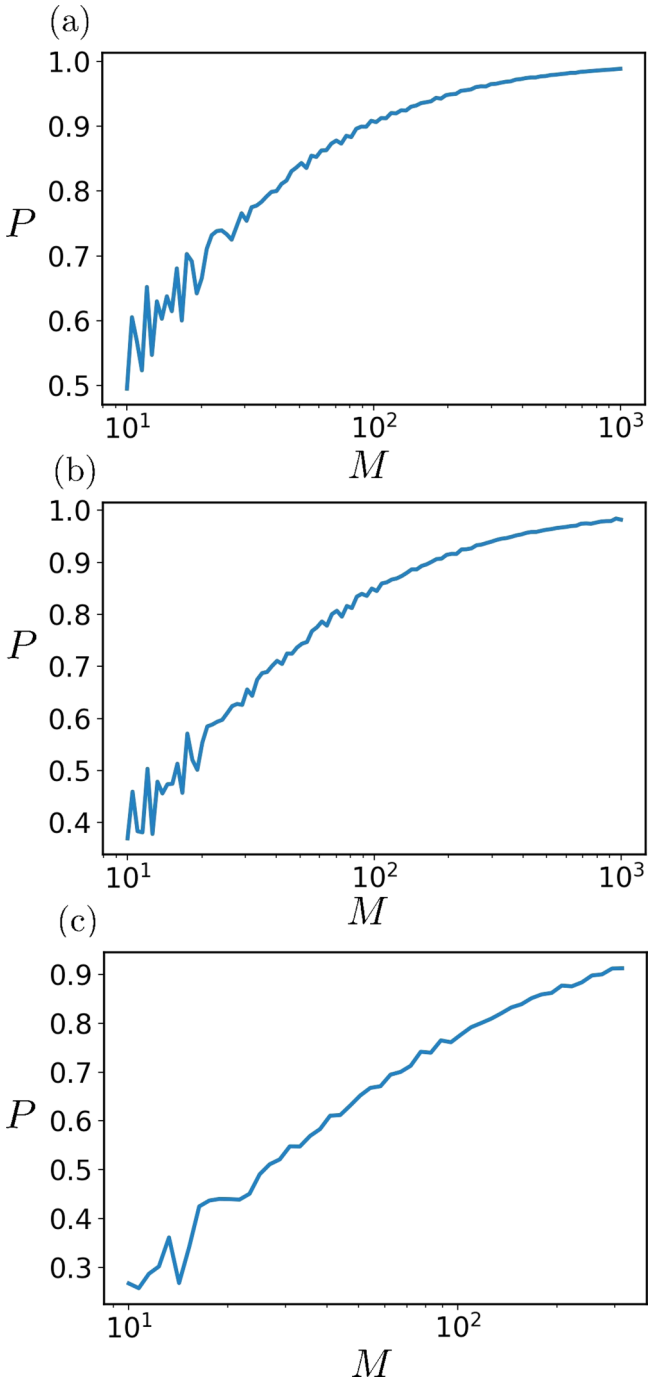

FIG. 15. Success probability versus M for high-order truncated M-simplex lattices. (a) Success probability with a four-stage search process on a third-order truncated M-simplex lattice. (b) Success probability with a five-stage search process on a fourth-order truncated M-simplex lattice. (c) Success probability with a six-stage search process on a fifth-order truncated M-simplex lattice.

From this, the Hamiltonian in the invariant subspace can be written down straightforwardly.

APPENDIX B: SUCCESS PROBABILITY OF A SEARCH ON A HIGHER-ORDER M-TRUNCATED SIMPLEX LATTICE

We recursively write the adjacency matrix in the subspace for a higher-order truncated M-simplex lattice. The

calculation in this Appendix is based on the assumption that the marked vertex is in the outermost layer of the graph. Since different locations of the marked vertex will not affect the algorithm for a second-order truncated simplex lattice as mentioned in the text, we conjecture that similar results could be obtained even if the marked vertex is in other locations for higher-order cases. With the search scheme proposed in Sec. II, for an rth-order truncated M-simplex lattice, we now consider the success probability of the search scheme with $(r+1)$ stages. The jumping rates are chosen as $\gamma = \frac{r+1}{M}, \frac{r}{M}, \ldots, \frac{2}{M}, \frac{1}{M}$, and the run time in each stage is chosen as $t = \pi M^{\frac{2r+1}{2}}/(2r+2), \pi M^{\frac{2r-1}{2}}/(2r), \ldots, \pi M^{\frac{3}{2}}/4, \pi M^{\frac{1}{2}}/2$ from stage 1 to stage $r+1$. We explicitly calculate the resulting success probability of the scheme on third-, fourth-, and fifth-order truncated M-simplex lattices. The results are shown in Fig. 15. As the size of the matrix representing the Hamiltonian increases very rapidly even in the subspace, the numerical process of directly calculating the evolution operators e^{-iHt} and applying them to the initial states becomes difficult for orders higher than the fifth. Actually even for a fifth-order lattice, the matrix size is larger than 1000×1000. And the largest and smallest matrix elements exhibit a very high ratio, which easily makes the numerical calculation unstable. (Our code is no longer stable for $M > 300$ on the fifth-order lattice. Especially, e^{-iHt} numerically calculated by our code is no longer unitary for the Hermitian Hamiltonian considered in our discussion.) But we believe that a high success probability should still be achievable on a truncated simplex latticeof higher than fifth order with our scheme.

[1] D. Dhar, J. Math. Phys. (NY) **18**, 577 (1977).
[2] D. Dhar, J. Math. Phys. **19**, 5 (1978).
[3] S. Kumar and Y. Singh, Phys. Rev. A **42**, 7151 (1990).
[4] S. Kumar and Y. Singh, J. Stat. Phys. **89**, 981 (1997).
[5] S. Kumar and Y. Singh, Phys. Rev. E **51**, 579 (1995).
[6] S. Kumar and Y. Singh, J. Phys. A: Math. Gen. **26**, L987 (1993).
[7] S. Kumar, Physica A: Stat. Mech. Appl. **292**, 422 (2001).
[8] C. T. Hill, Phys. Rev. D **67**, 085004 (2003).
[9] A. M. Childs and J. Goldstone, Phys. Rev. A **70**, 022314 (2004).
[10] D. A. Meyer and T. G. Wong, Phys. Rev. Lett. **114**, 110503 (2015).
[11] T. G. Wong and P. Philipp, Phys. Rev. A **94**, 022304 (2016).
[12] T. G. Wong, Phys. Rev. A **92**, 032320 (2015).
[13] T. G. Wong, Quantum Info. Process. **15**, 1411 (2016).
[14] Y. Aharonov, L. Davidovich, and N. Zagury, Phys. Rev. A **48**, 1687 (1993).
[15] S. E. Venegas-Andraca, Quantum Info. Process. **11**, 1015 (2012).
[16] J. Kempe, Contemp. Phys. **44**, 307 (2003).
[17] A. M. Childs, Phys. Rev. Lett. **102**, 180501 (2009).
[18] N. B. Lovett, S. Cooper, M. Everitt, M. Trevers, and V. Kendon, Phys. Rev. A **81**, 042330 (2010).
[19] A. M. Childs, D. Gosset, and Z. Webb, Science **339**, 791 (2013).
[20] E. Farhi and S. Gutmann, Phys. Rev. A **58**, 915 (1998).
[21] N. Shenvi, J. Kempe, and K. Birgitta Whaley, Phys. Rev. A **67**, 052307 (2003).
[22] M. Mohseni, P. Rebentrost, S. Lloyd, and A. Aspuru-Guzik, J. Chem. Phys **129**, 174106 (2008).
[23] C. Robens, W. Alt, D. Meschede, C. Emary, and A. Alberti, Phys. Rev. X **5**, 011003 (2015).
[24] Y.-C. Jeong, C. Di Franco, H.-T. Lim, M. Kim, and Y.-H. Kim, Nat. Commun. **4**, 2471 (2013).
[25] E. Flurin, V. V. Ramasesh, S. Hacohen-Gourgy, L. S. Martin, N. Y. Yao, and I. Siddiqi, Phys. Rev. X **7**, 031023 (2017).
[26] L. Xiao *et al.*, Nat. Phys. **13**, 1117 (2017).
[27] L. K. Grover, Phys. Rev. Lett. **79**, 325 (1997).
[28] J. Janmark, D. A. Meyer, and T. G. Wong, Phys. Rev. Lett. **112**, 210502 (2014).
[29] P. Philipp, L. Tarrataca, and S. Boettcher, Phys. Rev. A **93**, 032305 (2016).
[30] S. Chakraborty, L. Novo, A. Ambainis, and Y. Omar, Phys. Rev. Lett. **116**, 100501 (2016).
[31] L. Novo, S. Chakraborty, M. Mohseni, H. Neven, and Y. Omar, Sci. Rep. **5**, 13304 (2015).
[32] T. G. Wong, J. Phys. A: Math. Theor. **49**, 195303 (2016).
[33] E. Agliari, A. Blumen, and O. Mülken, Phys. Rev. A **82**, 012305 (2010).
[34] W. Carlson, A. Ford, E. Harris, J. Rosen, C. Tamon, and K. Wrobel, Quantum Info. Comput. **7**, 738 (2007).
[35] M. Christandl, N. Datta, A. Ekert, and A. J. Landahl, Phys. Rev. Lett. **92**, 187902 (2004).
[36] Z. Zimboras, M. Faccin, Z. Kadar, J. Whitfield, B. Lanyon, and J. Biamonte, Sci. Rep. **3**, 2361 (2013).
[37] T. G. Wong and A. Ambainis, Phys. Rev. A **92**, 022338 (2015).
[38] Y. Wang, S. Wu, and W. Wang, Phys. Rev. Research **1**, 033016 (2019).
[39] E. Farhi and S. Gutmann, Phys. Rev. A **57**, 2403 (1998).
[40] T. G. Wong, Quantum Info. Process. **14**, 1767 (2015).